

Rhodanine-Based Chromophores – Fast Access to Capable Photoswitches and Application in Light-Induced Apoptosis

Laura Köttner,^{a§} Friederike Wolff,^{b§} Peter Mayer,^c Esther Zanin,^{b} Henry Dube^{a*}*

^a Friedrich-Alexander-Universität Erlangen-Nürnberg, Department of Chemistry and Pharmacy, Nikolaus-Fiebiger-Str. 10, 91058 Erlangen, Germany.

^b Friedrich-Alexander-Universität Erlangen-Nürnberg, Department of Biology, Staudtstrasse 5, 91058 Erlangen, Germany.

^c Ludwig-Maximilians-Universität München, Department für Chemie and Munich Center for Integrated Protein Science CIPSM, D-81377 Munich, Germany.

[§] both authors contributed equally to this work

* corresponding authors: esther.zanin@fau.de and henry.dube@fau.de

Abstract

Molecular photoswitches are highly desirable in all chemistry-related areas of research. They provide effective outside control over geometric and electronic changes at the nanoscale using an easy to control and waste-free stimulus. However, simple and effective access to such molecular tools is typically not granted and elaborate syntheses and substitution schemes are needed in order to obtain efficient photoswitching properties. Here we present a series of rhodanine-based photoswitches that are prepared in one simple synthetic step without requiring elaborate purification. Photoswitching is induced by UV and visible light in both switching directions and thermal stabilities of the metastable states are high. An additional benefit is the hydrogen bonding capacity of the rhodanine fragment, which enables applications in supramolecular or medicinal chemistry. We further show that the known rhodanine-based inhibitor SMI-16a is a photoswitchable apoptosis inducer. The activity of SMI-16a can be switched ON or OFF by reversible photoisomerization between the inactive *E* and the active *Z* isomer. Rhodanine-based photoswitches therefore represent an easy to access and highly valuable molecular toolbox for implementing light responsiveness to functional molecular systems.

Introduction

Molecular photoswitches^[1] are versatile tools to control the behavior of matter at the nano-scale by light stimuli. Applications cover vast areas of research from molecular machines,^[2] to smart materials,^[3] catalysis^[4] or photopharmacology.^[5] Key to this success is oftentimes the precise control of photoswitch geometry and double bond isomerizing systems are frequently employed for this purpose. Stilbene^[6] and azobenzene^[7] based photoswitches represent probably the best-known examples but more recently other molecular core structures^[8] such as Stenhouse adducts,^[9] hydrazones,^[10] imidazole-biradicals,^[11] or hemipiperazine^[12] have emanated. Indigoid chromophores^[13] represent another different option for double bond isomerizing photoswitches. They undergo predictable changes in their geometry and are able to use visible light of different colors for both *Z* to *E* and *E* to *Z* photoisomerizations. The favorable photochemistry and synthetic versatility of indigoid chromophores have allowed their application in many different functional areas, giving rise to unique light controlled molecular machines,^[14] chiroptical switches,^[15] supramolecular systems,^[16] or biological^[17] or photopharmacology tools^[18] - to name just a few examples. A recent survey has further emphasized the potential of hemiindigoid chromophores as photopharmacological tool that still lies dormant.^[19]

In this work we present a new class of related, yet distinctive photoswitches with unique potential for applications especially in biomedical context. Rhodanine-based^[20] photoswitches inherit parts of the hemithioindigo (HTI) motive^[21] but the benzannulated thioindigo-fragment is replaced with a rhodanine or oxo-rhodanine unit to which the stilbene fragment is connected (Figure 1a). A simple one-step condensation of rhodanine and an aldehyde^[22] provides access to a large number of derivatives, which usually do not require column chromatography for purification. The thus obtained structures are well established motives in different areas of research such as fluorophore design,^[23] ion sensing,^[24] solar-cell dyes^[25] or medicinal and biological chemistry.^[26] For example, a number of widely used kinase inhibitors such as SMI-16a^[27] or SMI-4a^[27-28] with activity against PIM kinases (proviral integrations of moloney virus)^[28-29] are based on this structural motive. Despite this great versatility, to the best of our knowledge the capacity for photoswitching in this class of structures has not been investigated so far.

Here we show, that rhodanine chromophores are capable photoswitches with strongly tunable property profiles allowing to tailor them for particular applications (Figure 1). Thermal stability of metastable states can be precisely modulated by simply changing from the highly bistable oxo-rhodanine structures to the sulfur-substituted rhodanines. At the same time a significant

red-shift of the absorption is observed for the latter. By introducing further heterocyclic structures, which have recently been shown effective in enhancing photoswitching of HTI chromophores, strongly improved properties are obtained. These include enhanced photochromism, near quantitative switching, and improved thermal bistability. The additional benefits of increased hydrogen bonding capacities are not only of interest for biomedical applications but also for supramolecular interactions, implementation into materials or molecular sensing, and recognition purposes. Finally, it is shown here that the known PIM kinase inhibitor SMI-16a (derivative **1**) is in itself a capable photopharmacology tool, which allows reversible photocontrol over apoptosis in cancer cells. PIM kinase is a promising drug target for cancer therapy and plays a central role in multiple cell cycle and apoptotic pathways.^[30] A related rhodanine variant (derivative **5**) is also active in its *Z*-isomeric form and shows a pronounced red-shifted absorption. These findings thus open up a facile avenue to a plethora of capable light responsive tools enabling the manipulation of molecular phenomena and biological functions by light.

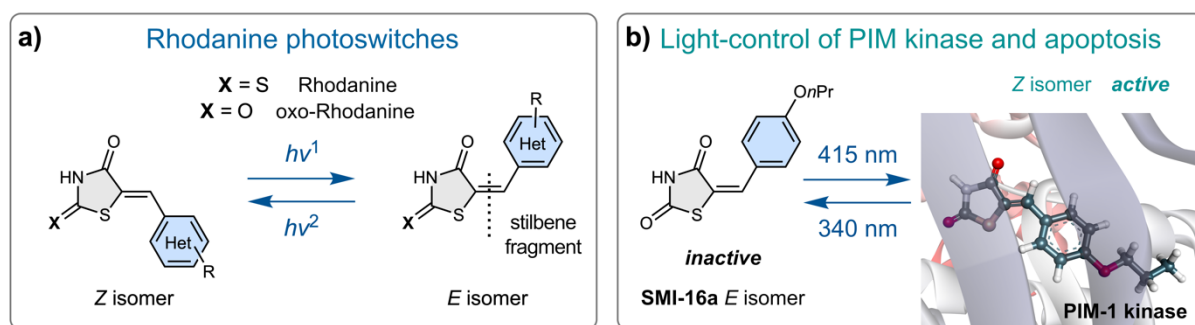


Figure 1 Rhodanine and oxo-rhodanine-based chromophores for visible light responsive photoswitching. a) Rhodanine-based photoswitches. b) Application of rhodanines as photopharmacological tool allowing light-control of apoptosis via isomer selective PIM kinase inhibition. Image on the right side shows the *Z* isomer in the active site of PIM-1 kinase.

Results and Discussion

In this study we investigated 14 different rhodanine chromophores for their photoswitching capacity (Figure 2). These include four derivatives **1-4** bearing an oxo-rhodanine fragment and 10 derivatives **5-14** bearing a rhodanine fragment. Variations at the stilbene fragment include electron neutral, electron rich, and electron deficient benzenes as well as different imidazole and indole heterocycles, which have recently been shown to enable superior photoswitch

properties in HTIs.^[31] For direct comparison of the effect of variation at the X-position (oxygen in oxo-rhodanines and sulfur in rhodanines) derivatives **1-4** were matched with **5-8**.

Synthesis of rhodanine-based chromophores proceeds in one step from commercially available starting materials, i.e. oxo-rhodanine or rhodanine and different aromatic aldehydes. The reaction can be conducted neat at higher temperatures (typically 110 °C) using urea to facilitate the reaction as described previously.^[22] In case the mixture is not liquifying under the reaction conditions, which prevents proper mixing, the reaction can also be done in methanol solution at 60 °C. After short heating times the reaction mixtures turn colorful - depending on the aldehyde used - yellow to purple colors are observed signifying product formation. Typically, good to very good yields are obtained for the different products, which can be isolated in pure form by a simple filtration and washing/recrystallization procedure omitting workup, extraction, and chromatography (for details see the Supporting Information). In this way, the 14 different rhodanine-based photoswitches **1-14** (Figure 2a) were prepared in up to 98% yield. After crystallization, the structures of pure *Z* isomers of compounds **5-7** and **11** could be obtained by single crystal X-ray diffraction (Figure 2b) evidencing the expected constitutions.

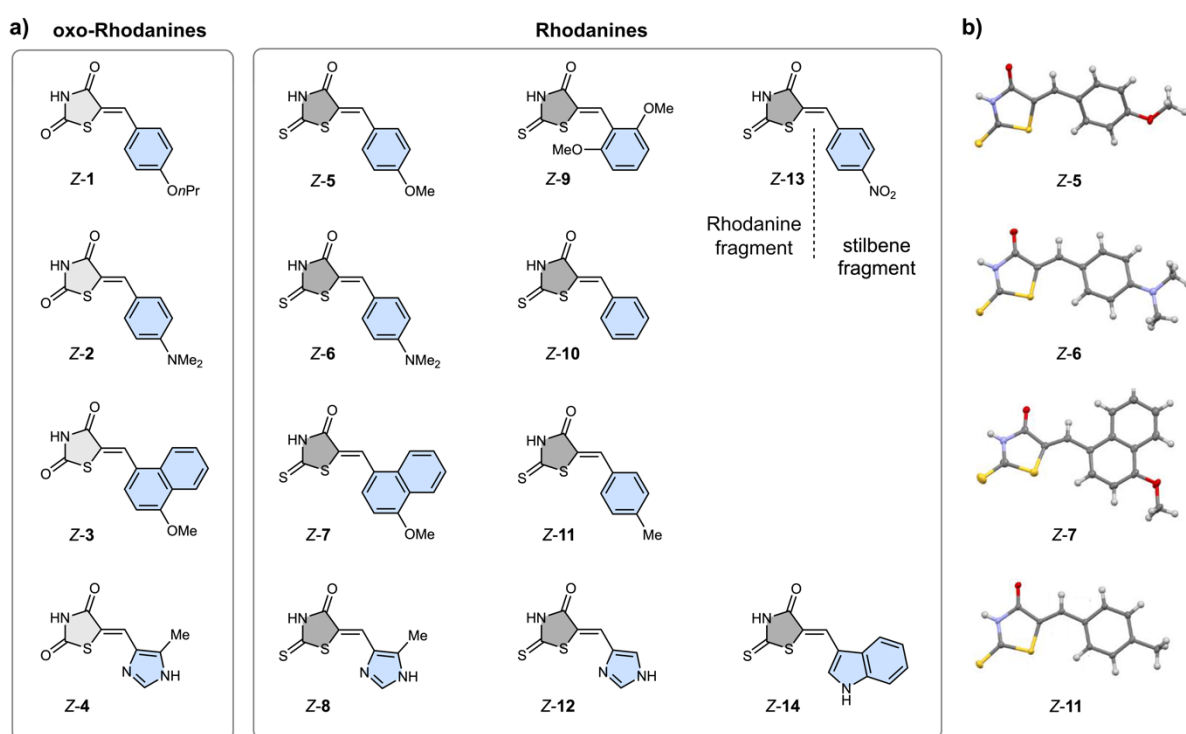


Figure 2 Molecular structures of oxo-rhodanine- and rhodanine-based chromophores **1-14** investigated in this study. a) The thermodynamically most stable *Z* isomers are shown schematically. b) Structures of derivatives **5-7** and **11** in their *Z* isomeric configuration in the crystalline state.

The thermal properties of rhodanine-based photoswitches **1-14** were scrutinized first to establish stabilities of the metastable states in different solvents in the dark (for a summary of measured half-lives at various temperatures see Table 1). Both oxo- and rhodanine-based photoswitches seem not to thermally interconvert via simple first order reaction but rather by more complex processes. At present the origin of this behavior is not known but seems to involve aggregation processes and will be investigated in more detail in the future. Therefore, no *Gibbs* energies of activation were calculated and only half-life times were taken into consideration when comparing thermal stabilities. Nevertheless, clear trends are observed upon thermal isomerization. In all cases the *Z* isomer is thermodynamically most stable rendering the *E* isomer metastable. Typically, complete thermal conversion to the *Z* isomer takes place upon heating. Thermal *E* to *Z* isomerization proceeds slowly for all photoswitches with half-lives ranging from hours to days at 55 °C (THF-*d*₈ solution) for photoswitches **5, 6, 7, 11, and 13** and at 85 °C (dioxane-*d*₈ solution) for the remaining derivatives depending on the particular substitution. In 1% DMSO/PBS buffer solution thermal stability is diminished but still thermal half lives in the range of minutes to several hours at 37 °C are retained (see Figure 4a and the Supporting Information for details). A consistent trend is observed when comparing oxo-rhodanines **1-4** with the corresponding rhodanines **5-8**, in which the former exhibit significantly higher thermal stabilities of the metastable *E* isomers. With these thermal stabilities (oxo)-rhodanine-based chromophores are well competitive with other capable photoswitches such as azobenzenes or HTI.

With pronounced thermal stabilities established, the photophysical and photochemical properties were quantified next (Table 1). Measured molar absorption coefficients reveal narrow absorption bands in the UV and/or visible part of the electromagnetic spectrum for all rhodanine-based photoswitches **1** to **14**. The rhodanine chromophores show a significant bathochromic shift of their absorptions (reaching up to 57 nm) when compared to the corresponding oxo-rhodanine-based derivatives (see Figure 3a and b for examples and also the Supporting Information). Further bathochromic shifts can be achieved by introducing electron donating substituents at the stilbene fragments or by heterocycle substitution. With the exception of derivative **9** all rhodanine-based photoswitches **1** to **14** exhibit positive photochromism with bathochromic shift of the absorption for the metastable *E* isomer. The absolute difference in absorption between *E* and *Z* isomers is not very large for benzene-substituted derivatives but is much more pronounced for heterocyclic derivatives **4, 8, 12, and**

14. Consequently, photoswitching for the former is not complete in the *Z* to *E* isomerization direction and a maximum of 68% of *E* isomer can be accumulated in the photostationary state (pss). For many applications such performance is still effective, especially if threshold effects or bulk responses are intended. However, photoisomerization of heterocyclic derivatives **4** and **8** yields significantly higher yields of the *E* isomer beyond 80% (Figure 3c). For all derivatives except **9** the corresponding *E* to *Z* photoisomerizations are more pronounced yielding the *Z* isomer in >85% in the pss. For heterocyclic derivatives **4** and **8** even quantitative conversion is achieved (Figure 3c). In case of derivatives **2** and **6** to **14** photoswitching in both switching directions can be conducted using visible light instead of UV light, which adds another advantage to this class of chromophores. To test the influence of the solvent, THF with intermediate polarity and non-protic nature as well as methanol with high polarity and protic nature were chosen (see Supporting Information for all conditions tested). For the known inhibitor SMI-16a – i.e. derivative **1** – as well as **5**, and **8** also photoswitching experiments in buffer solution and cell-media were performed (see Figure 4b and Supporting Information). For benzene-substituted derivatives the effects of solvent changes on the photoswitching capacity are very small and also buffer and cell media environments do not lead to deterioration of performance. In the case of heterocyclic derivatives, a somewhat diminished completeness for the *Z* to *E* photoisomerization direction in protic media is seen for **8**.

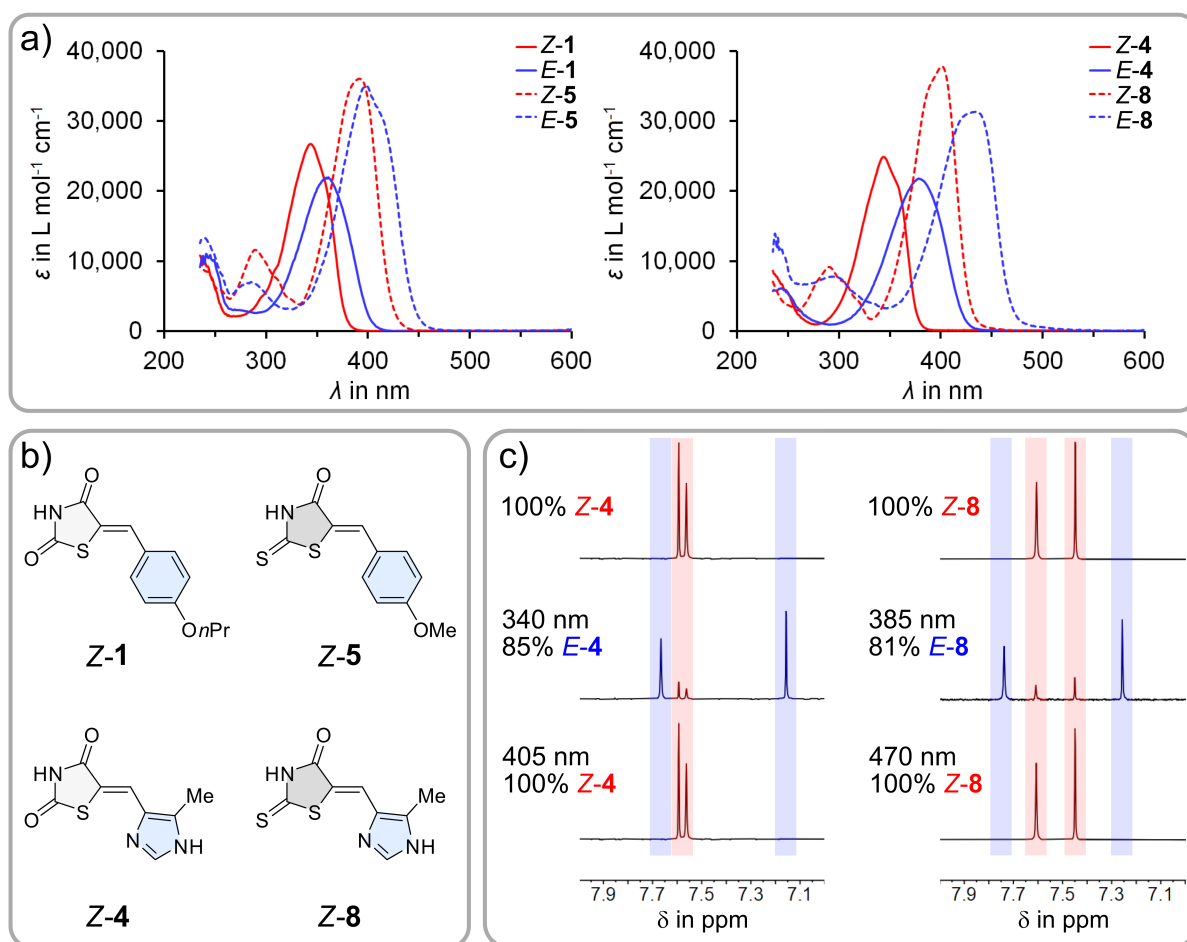


Figure 3 Photoswitching properties of selected rhodanine-based chromophores. a) Absorption comparison of oxo-rhodanine with rhodanine photoswitches. Molar absorption coefficients are shown for both *Z* and *E* isomers of derivatives **1** and **5** as well as for **4** and **8** in THF solution. b) Schematic representation of rhodanine-based chromophores **1**, **4**, **5**, and **8**. c) Partial ^1H NMR spectra (400 MHz, $\text{THF-}d_8$, 23°C) showing light induced isomer interconversions from top to bottom for **4** and **8**.

Taken together these results showcase that both oxo-rhodanine and rhodanine-based chromophores represent capable photoswitches the properties of which can be tuned in a wide range by different substitutions at the rhodanine or the stilbene fragment. Best performances are given by imidazole and indole incorporating **4**, **8**, **12**, and **14**. These derivatives combine high isomer enrichment in the pss, pronounced photochromism, visible light responsiveness at least for one switching direction, and high thermal stabilities of metastable states.

Table 1 Photochemical and photophysical properties of (oxo)-rhodanine-based photoswitches for indicated solvents and temperatures.

(oxo)-rhodanine	λ_{\max} ; ϵ of <i>Z/E</i> isomers most redshifted abs. / nm; L mol ⁻¹ cm ⁻¹ in THF- <i>d</i> ₈ or *in 1% DMSO/PBS buffer	isomer yield in pss / % (nominal LED) in THF- <i>d</i> ₈ or *in 1% DMSO/PBS buffer	ΔG / kcal mol ⁻¹ (solvent)	$t_{1/2}$ / h (T, solvent)
1	344; 26,700	57% <i>E</i> (340 nm)	≥ 2.0	114 (85 °C, dioxane- <i>d</i> ₈)
	361; 22,000	99% <i>Z</i> (405 nm)	(dioxane- <i>d</i> ₈)	
	*347; 26,000	*61% <i>E</i> (340 nm)		
	*358; 16,600	*93% <i>Z</i> (405 nm)		
2	401; 36,200	53% <i>E</i> (405 nm)	≥ 0.6	138 (85 °C, dioxane- <i>d</i> ₈)
	419; 32,300	98% <i>Z</i> (470 nm)	(dioxane- <i>d</i> ₈)	
3	374; 19,200	68% <i>E</i> (365 nm)	≥ 0.3	≥ 480 (85 °C, dioxane- <i>d</i> ₈)
	392; 12,700	97% <i>Z</i> (450 nm)	(dioxane- <i>d</i> ₈)	
4	344; 29,900	85% <i>E</i> (365 nm)	no	no isomerization (85 °C, dioxane- <i>d</i> ₈)
	378; 21,800	100% <i>Z</i> (405 nm)	isomerization	
5	392; 36,100	52% <i>E</i> (385 nm)	≥ 2.0	30 (55 °C, THF- <i>d</i> ₈)
	397; 35,000	86% <i>Z</i> (420 nm)	(THF- <i>d</i> ₈)	
	*396; 33,900	*65% <i>E</i> (385 nm)		
	*404; 27,500	*86% <i>Z</i> (470 nm)		
6	455; 45,300	52% <i>E</i> (420 nm)	≥ 2.0	7 (55 °C, THF- <i>d</i> ₈)
	474; 51,500	89% <i>Z</i> (505 nm)	(THF- <i>d</i> ₈)	
7	414; 25,900	62% <i>E</i> (385 nm)	≥ 2.0	143 (55 °C, THF- <i>d</i> ₈)
	428; 21,200	90% <i>Z</i> (470 nm)	(THF- <i>d</i> ₈)	
8	401; 37,800	81% <i>E</i> (385 nm)	≥ 1.7	95 (85 °C, dioxane- <i>d</i> ₈)
	435; 31,300	100% <i>Z</i> (470 nm)	(dioxane- <i>d</i> ₈)	
	*404; 33,600	*75% <i>E</i> (385 nm)		
	*419; 32,300	*89% <i>Z</i> (470 nm)		
9	384; 29,500	68% <i>E</i> (385 nm)	≥ 2.0	101 (85 °C, dioxane- <i>d</i> ₈)
	373; 17,900	44% <i>Z</i> (340 nm)	(dioxane- <i>d</i> ₈)	
10	344; 26,700	49% <i>E</i> (365 nm)	≥ 2.0	85 (85 °C, dioxane- <i>d</i> ₈)
	375; 32,800	88% <i>Z</i> (420 nm)	(dioxane- <i>d</i> ₈)	
11	382; 38,400	53% <i>E</i> (365 nm)	≥ 2.0	19 (55 °C, dioxane- <i>d</i> ₈)

	382; 35,400	91% <i>Z</i> (420 nm)	(THF- <i>d</i> ₈)	THF- <i>d</i> ₈)
12	388; 37,300	70% <i>E</i> (365 nm)	≥2.0	110 (85 °C,
	408; 33,800	94% <i>Z</i> (415 nm)	(dioxane- <i>d</i> ₈)	dioxane- <i>d</i> ₈)
13	377; 34,500	45% <i>E</i> (385 nm)	≥2.0	82 (55 °C,
	387; 30,500	85% <i>Z</i> (420 nm)	(THF- <i>d</i> ₈)	THF- <i>d</i> ₈)
14	433; 32,900	67% <i>E</i> (410 nm)	≥1.6	12 (85 °C,
	447; 39,00	92% <i>Z</i> (470 nm)	(dioxane- <i>d</i> ₈)	dioxane- <i>d</i> ₈)

To further showcase the potential of rhodanine-based photoswitches, we investigated the capacity for biological applications using the structure of known PIM kinase inhibitor SMI-16a – i.e. oxo-rhodanine **Z-1** – as inspiration. PIM kinases are oncogenes that are overexpressed in different types of cancer cells such as pancreatic cancer or acute myeloid leukemia. PIM kinases belong to the class of constitutively active kinases and they phosphorylate several proliferation promoting and anti-apoptotic master regulators such as c-myc and BAD (BCL-2 antagonist of cell death). The architecture of ATP binding sites of PIM kinases is unique in comparison to other kinases and therefore highly selective inhibition of PIM becomes possible. For these reasons PIM kinases are gaining increasing attention as promising pharmacological targets for specific cancer therapy.^[30, 32] The *Z* isomer of oxo-rhodanine **1** has been shown to selectively and strongly inhibit PIM-1 kinase.^[27] Upon PIM-1 inhibition, the non-phosphorylated target protein BAD inhibits the pro-survival protein BCLXL1 and apoptosis is induced.^[30b, 32] Additionally, inhibition of the related PIM-2 kinase by oxo-rhodanine **Z-1** has also been demonstrated, which furthers its impact as anti-cancer agent.^[29b]

In this biological context we have scrutinized the biological activity of rhodanine-based photoswitches **5** and **8** (Figure 4c and d). Derivative **5** was chosen for its close structural relation to **1** (bearing a sulfur instead of the oxygen at position X and a shorter alkyl-residue at the stilbene oxygen atom, i.e. methyl instead of *n*-propyl) but offering a significantly red-shifted absorption. Derivative **8** was chosen for its outstanding photoswitching properties retaining the rhodanine fragment as important PIM kinase binding motive.^[33] The thermodynamically stable *Z* isomers of **5** and **8** were tested in human cervix carcinoma HeLa cells by incubating them with 150 μM of the respective photoswitch. After 19 h incubation, cells were fixed and stained for DNA and F-actin and the total number of cells was determined. In these experiments it was revealed that *Z-5* shows biological activity and kills cancer cells with similar effectiveness as *Z-1* at 50 μM and 150 μM concentration (Figure 4c and d and Supporting Information; see below for further details on *Z-1* activity). Derivative *Z-8* however

did not show a promising biological activity and thus was not further scrutinized. With *Z*-**5** as biologically active agent we then set out to test the activity of its corresponding *E* isomer. However, the low thermal stability of *E*-**5** in buffer media did not allow us to examine its potency in the biological context (see Supporting Information for details). Despite the more favorable absorption properties of **5** in the visible region of the spectrum its poor photochromism also prevented a continuous irradiation approach to permanently enrich the *E* isomer upon bulk-photoisomerization of the *Z* isomer. Therefore, an effective photopharmacological application of **5** as light-controlled anti-cancer agent was hampered, however, its potency as prospective inhibitor of PIM kinases could be demonstrated for the *Z* isomer.

As discussed above, oxo-rhodanine **1** (SMI-16a) itself can be photoisomerized reversibly between the thermodynamically stable *Z* isomer (up to 93% under blue light irradiation of e.g. 405 nm wavelength) and the metastable *E* isomer (up to 61% under UV light irradiation of 340 nm) without disturbance of thermal *E* to *Z* isomerization (Figure 4a and b). Although the *Z* isomer is a known and commercially available inhibitor of PIM kinases^[27-28] the corresponding *E* isomer has not been scrutinized for its biological activity to the best of our knowledge. If the *E* isomer of **1** is in fact biologically inactive, an opportunity for light induced activation by blue light would present itself. The intrinsically very high thermal stability of the *E* isomer would for example allow a global administration and timed local activation scheme.

We have tested this hypothesis also in HeLa cells by incubating them with 150 μ M of pure SMI-16a *Z*-**1** or *E*-**1** isomer. Again, after 19 h incubation, cells were fixed and stained for DNA and F-actin and the total number of cells was determined. As expected, incubation with the *Z*-**1** isomer strongly reduced cell number (Figure 4c, d and e) due to induction of apoptosis.^[29b] To our delight, the corresponding *E*-**1** isomer did not decrease the cell number suggesting the *E*-**1** isomer is inactive (Figure 4c, d and e). This strong difference in activity of the *E* and *Z* isomer serves as foundation for light control of PIM kinase activity. To induce *E* to *Z* photoisomerization, the *E*-**1** isomer was irradiated with blue light in cell culture medium prior to the addition to cells. As a result, after 19 h the cell number was strongly reduced (Figure 4c, d and e), which was similar to the effect of the pure *Z*-**1** isomer addition. This shows that irradiation of *E*-**1** isomer results in highly efficient photoisomerization into the *Z*-**1** isomer. Thus, a light controlled ON switching and induction of apoptosis could be established with the oxo-rhodanine-based photoswitch **1**, showcasing its very high potential as molecular tool for medicinal chemistry. Also, the reverse behavior can be elicited by irradiating the *Z*-**1** isomer with 340 nm light in cell culture medium prior to adding it to the cells. The irradiation *Z*-**1**

isomer with 340 nm light leads to a significant recovery of cell viability and establishes reversible control of the biological PIM kinase function (Figure 4c, d and e).

Finally, also stability against glutathione was tested for derivatives **1**, **5**, and **8**. Over the course of 10 h no discernible change of absorption could be observed for 50 μm in 1/1 DMSO/PBS buffer solutions in the presence of 10 mM glutathione (see Supporting Information for experimental details). Thus, despite the presence of a Michael-acceptor system (oxo)-rhodanine photoswitches possess high stability against glutathione addition and are not expected to be quickly eliminated via such a mechanism within the cell.

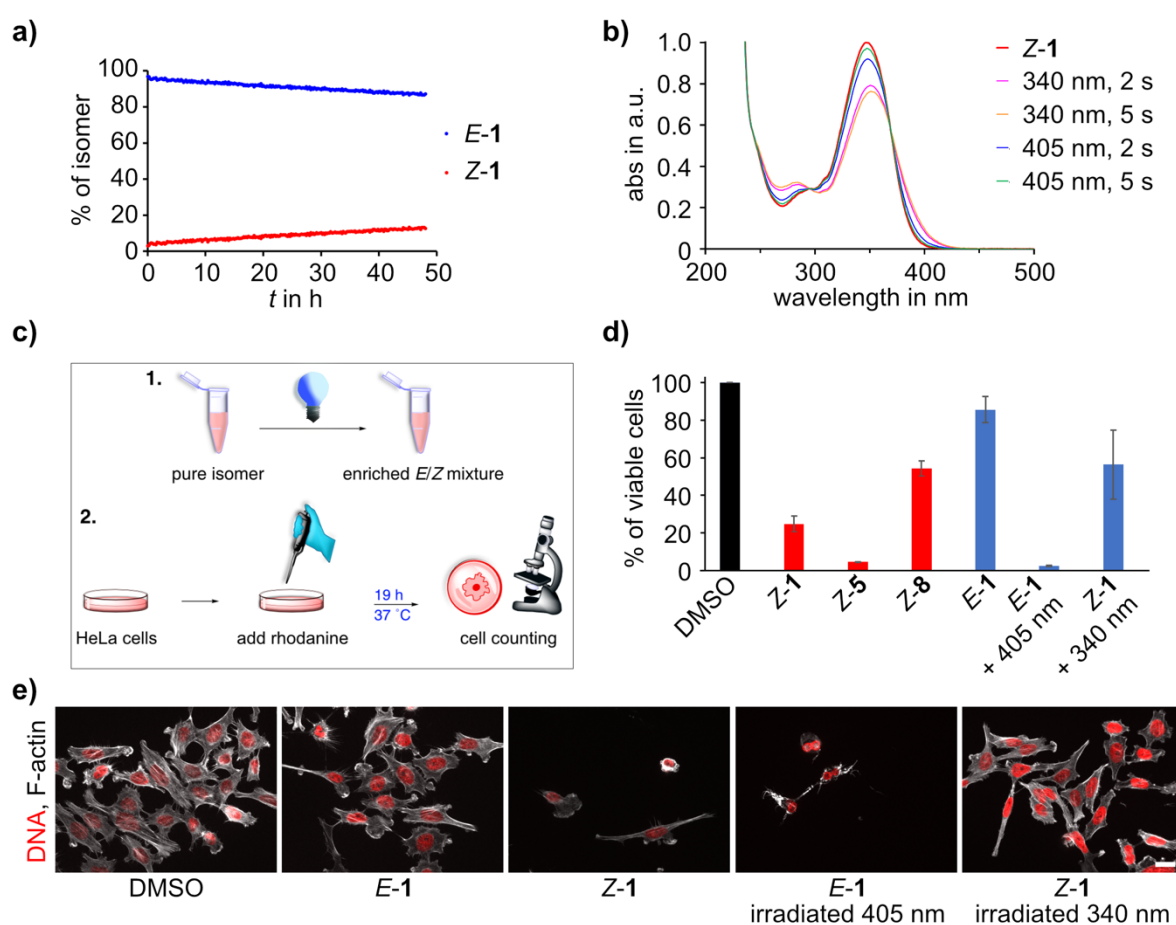


Figure 4 a) Thermal stability of *E-1* and *Z-1* in 1% DMSO/PBS buffer solution at 37 °C in the dark. b) Photoswitching of **1** in 1% DMSO/PBS buffer solution at 23 °C. c) Schematic representation of the experimental set up to test biomedical activity. Human cervix carcinoma cells (HeLa) were treated with the different compounds for 19 h and subsequently the cell number was determined. For selected conditions compounds were irradiated with the indicated wave lengths in cell culture medium for 10 min and afterwards added to the cells. d) Quantification of the % of viable cells for the indicated treatments. Error bars represent standard deviation and at least two independent

experiments were performed for each condition. e) Sample microscopy images of HeLa cells stained for DNA (red) and F-actin (white) for the indicated conditions. Scale bar 20 μm .

Conclusion

In conclusion we demonstrate that oxo-rhodanine and rhodanine chromophores are capable photoswitching motives for light induced double bond isomerizations reactions. A simple synthesis delivers fast access to a variety of different structures and thus allows to tune thermal and photochemical/photophysical properties in a wide range. The best performing photoswitches bear heterocyclic residues and deliver nearly quantitative photoisomerizations, strong photochromism, and high thermal stabilities of the metastable *E* isomers. Absorptions can be shifted up to 57 nm to the red by replacing one oxygen in oxo-rhodanines by sulfur. Thermal stability of the *E* isomers is lowered by this substitution, making the latter highly tunable by a simple one-atom replacement. The biological application of rhodanine-based photoswitch *Z-5* demonstrated induction of apoptosis with similar effectiveness as *Z-1* – i.e. the known PIM kinase inhibitor SMI-16a. Derivative *Z-1* itself was further shown to exhibit very pronounced photomodulation of its biological activity enabling light-induced apoptosis regulation. (Oxo)-rhodanine chromophores are thus shown to be highly promising photocontrollable molecular tools with especially potent applicability in biological and medicinal context.

Acknowledgements

H. Dube thanks the Deutsche Forschungsgemeinschaft (DFG) for an Emmy Noether fellowship (DU 1414/1-2). E. Zanin thanks the DFG for an Emmy Noether fellowship (ZA619/3) and Helmut Brandstätter and Renato Frischknecht for access and introduction to the Apoptom microscope. We further thank the Deutsche Forschungsgemeinschaft (SFB 749, A12) and the Cluster of Excellence “Center for Integrated Protein Science Munich” (CIPSM) for financial support. Open access funding enabled and organized by Projekt DEAL.

Keywords: photoswitch • rhodanine • photopharmacology • PIM kinase • apoptosis

References

- [1] a) *Molecular Photoswitches. Chemistry, Properties, and Applications*, Wiley-VCH, Weinheim, **2022**; b) B. L. Feringa, W. R. Browne, *Molecular Switches, Vol. 1*, Wiley-VCH, Weinheim, **2011**.
- [2] a) S. Kassem, T. van Leeuwen, A. S. Lubbe, M. R. Wilson, B. L. Feringa, D. A. Leigh, *Chem. Soc. Rev.* **2017**, *46*, 2592-2621; b) S. Erbas-Cakmak, D. A. Leigh, C. T. McTernan, A. L. Nussbaumer, *Chem. Rev.* **2015**, *115*, 10081-10206.
- [3] a) J. Boelke, S. Hecht, *Adv. Optical Mater.* **2019**, *7*, 1900404; b) A. Goulet-Hanssens, F. Eisenreich, S. Hecht, *Adv. Mater.* **2020**, *32*, e1905966; c) W. Danowski, T. van Leeuwen, W. R. Browne, B. L. Feringa, *Nanoscale Advances* **2021**, *3*, 24-40.
- [4] a) R. Göstl, A. Senf, S. Hecht, *Chem. Soc. Rev.* **2014**, *43*, 1982-1996; b) R. Dorel, B. L. Feringa, *Chem. Commun.* **2019**, *55*, 6477-6486.
- [5] a) J. Morstein, D. Trauner, *Curr. Opin. Chem. Biol.* **2019**, *50*, 145-151; b) K. Hull, J. Morstein, D. Trauner, *Chem. Rev.* **2018**, *118*, 10710-10747; c) M. M. Lerch, M. J. Hansen, G. M. van Dam, W. Szymanski, B. L. Feringa, *Angew. Chem. Int. Ed.* **2016**, *55*, 10978-10999.
- [6] a) D. H. Waldeck, *Chem. Rev.* **1991**, *91*, 415-436; b) D. Villaron, S. J. Wezenberg, *Angew. Chem. Int. Ed.* **2020**, *59*, 13192-13202.
- [7] a) H. M. Bandara, S. C. Burdette, *Chem. Soc. Rev.* **2012**, *41*, 1809-1825; b) F. A. Jerca, V. V. Jerca, R. Hoogenboom, *Nat. Rev. Chem.* **2022**, *6*, 51-69.
- [8] J. D. Harris, M. J. Moran, I. Aprahamian, *Proc. Natl. Acad. Sci. U. S. A.* **2018**, *115*, 9414-9422.
- [9] a) S. Helmy, F. A. Leibfarth, S. Oh, J. E. Poelma, C. J. Hawker, J. Read de Alaniz, *J. Am. Chem. Soc.* **2014**, *136*, 8169-8172; b) H. Zulfikri, M. A. J. Koenis, M. M. Lerch, M. Di Donato, W. Szymanski, C. Filippi, B. L. Feringa, W. J. Buma, *J. Am. Chem. Soc.* **2019**, *141*, 7376-7384.
- [10] a) Y. Yang, R. P. Hughes, I. Aprahamian, *J. Am. Chem. Soc.* **2012**, *134*, 15221-15224; b) Y. Yang, R. P. Hughes, I. Aprahamian, *J. Am. Chem. Soc.* **2014**, *136*, 13190-13193; c) B. Shao, I. Aprahamian, *Chem* **2020**, *6*, 2162-2173; d) D. J. van Dijken, P. Kovaricek, S. P. Ihrig, S. Hecht, *J. Am. Chem. Soc.* **2015**, *137*, 14982-14991.
- [11] a) K. Mutoh, Y. Nakagawa, A. Sakamoto, Y. Kobayashi, J. Abe, *J. Am. Chem. Soc.* **2015**, *137*, 5674-5677; b) K. Mutoh, Y. Kobayashi, T. Yamane, T. Ikezawa, J. Abe, *J. Am. Chem. Soc.* **2017**, *139*, 4452-4461.

- [12] S. Kirchner, A. L. Leistner, P. Godtel, A. Seliwjorstow, S. Weber, J. Karcher, M. Nieger, Z. Pianowski, *Nat. Commun.* **2022**, *13*, 6066.
- [13] a) T. Bartelmann, H. Dube, in *Molecular Photoswitches*, **2022**, pp. 283-302; b) C. Y. Huang, A. Bonasera, L. Hristov, Y. Garmshausen, B. M. Schmidt, D. Jacquemin, S. Hecht, *J. Am. Chem. Soc.* **2017**, *139*, 15205-15211; c) S. Thumser, L. Kottner, N. Hoffmann, P. Mayer, H. Dube, *J. Am. Chem. Soc.* **2021**, *143*, 18251-18260; d) F. Kohl, A. Gerwien, F. Hampel, P. Mayer, H. Dube, *J. Am. Chem. Soc.* **2022**, *144*, 2847-2852.
- [14] a) M. Guentner, M. Schildhauer, S. Thumser, P. Mayer, D. Stephenson, P. J. Mayer, H. Dube, *Nat. Commun.* **2015**, *6*, 8406; b) A. Gerwien, P. Mayer, H. Dube, *J. Am. Chem. Soc.* **2018**, *140*, 16442-16445; c) A. Gerwien, P. Mayer, H. Dube, *Nat. Commun.* **2019**, *10*, 4449; d) E. Uhl, P. Mayer, H. Dube, *ChemRxiv* **2019**, doi: 10.26434/chemrxiv.10048871.v10048871; e) N. N. Bach, V. Josef, H. Maid, H. Dube, *Angew. Chem. Int. Ed.* **2022**, *61*, e202201882; f) A. Gerwien, F. Gnannt, P. Mayer, H. Dube, *Nat. Chem.* **2022**, *14*, 670-676; g) D. Roke, M. Sen, W. Danowski, S. J. Wezenberg, B. L. Feringa, *J. Am. Chem. Soc.* **2019**, *141*, 7622-7627.
- [15] C. Petermayer, H. Dube, *J. Am. Chem. Soc.* **2018**, *140*, 13558-13561.
- [16] a) S. Wiedbrauk, T. Bartelmann, S. Thumser, P. Mayer, H. Dube, *Nat. Commun.* **2018**, *9*, 1456; b) K. Grill, H. Dube, *J. Am. Chem. Soc.* **2020**, *142*, 19300-19307.
- [17] a) T. Lougheed, V. Borisenko, T. Hennig, K. Rück-Braun, G. A. Woolley, *Org. Biomol. Chem.* **2004**, *2*, 2798-2801; b) S. Herre, T. Schadendorf, I. Ivanov, C. Herrberger, W. Steinle, K. Rück-Braun, R. Preissner, H. Kuhn, *ChemBioChem* **2006**, *7*, 1089-1095; c) T. Cordes, C. Elsner, T. T. Herzog, C. Hoppmann, T. Schadendorf, W. Summerer, K. Rück-Braun, W. Zinth, *Chemical Physics* **2009**, *358*, 103-110; d) N. Regner, T. T. Herzog, K. Haiser, C. Hoppmann, M. Beyermann, J. Sauermann, M. Engelhard, T. Cordes, K. Rück-Braun, W. Zinth, *J. Phys. Chem. B* **2012**, *116*, 4181-4191.
- [18] a) A. Sailer, F. Ermer, Y. Kraus, F. H. Lutter, C. Donau, M. Bremerich, J. Ahlfeld, O. Thorn-Seshold, *ChemBioChem* **2019**, *20*, 1305-1314; b) A. Sailer, J. C. M. Meiring, C. Heise, L. N. Pettersson, A. Akhmanova, J. Thorn-Seshold, O. Thorn-Seshold, *Angew. Chem. Int. Ed.* **2021**, *60*, 23695-23704.
- [19] L. M. Lazinski, G. Royal, M. Robin, M. Maresca, R. Haudecoeur, *J. Med. Chem.* **2022**, *65*, 12594-12625.

- [20] a) F. C. Brown, *Chem. Rev.* **1961**, *61*, 463-521; b) S. P. Singh, S. S. Parmar, K. Raman, V. I. Stenberg, *Chem. Rev.* **1981**, *81*, 175-203.
- [21] S. Wiedbrauk, H. Dube, *Tetrahedron Lett.* **2015**, *56*, 4266-4274.
- [22] S. Shah, B. Singh, *Bioorg. Med. Chem. Lett.* **2012**, *22*, 5388-5391.
- [23] Z. Li, B. Huang, Y. Wang, W. Yuan, Y. Wu, R. Yu, G. Xing, T. Zou, Y. Tao, *RSC Adv* **2020**, *11*, 160-163.
- [24] D. B. Christopher Leslee, S. Karuppannan, M. V. Karmegam, S. Gandhi, S. Subramanian, *J. Fluoresc.* **2019**, *29*, 75-89.
- [25] a) H. Liu, Z. a. Li, D. Zhao, *Science China Materials* **2019**, *62*, 1574-1596; b) B. Moll, T. Tichelkamp, S. Wegner, B. Francis, T. J. J. Muller, C. Janiak, *RSC Adv* **2019**, *9*, 37365-37375; c) D. Madrid-Usuga, C. A. Melo-Luna, A. Insuasty, A. Ortiz, J. H. Reina, *J. Phys. Chem. A* **2018**, *122*, 8469-8476; d) T. Meyer, D. Ogermann, A. Pankrath, K. Kleinermanns, T. J. Muller, *J. Org. Chem.* **2012**, *77*, 3704-3715.
- [26] a) S. M. Mousavi, M. Zarei, S. A. Hashemi, A. Babapoor, A. M. Amani, *Artificial Cells, Nanomedicine, and Biotechnology* **2019**, *47*, 1132-1148; b) M. Tarahomi, R. Baharfar, M. Mohseni, *Clinical Microbiology and Infectious Diseases* **2019**, *4*; c) B. T. Moorthy, S. Ravi, M. Srivastava, K. K. Chiruvella, H. Hemlal, O. Joy, S. C. Raghavan, *Bioorg. Med. Chem. Lett.* **2010**, *20*, 6297-6301.
- [27] Z. Beharry, M. Zemsanova, S. Mahajan, F. Zhang, J. Ma, Z. Xia, M. Lilly, C. D. Smith, A. S. Kraft, *Mol. Cancer Ther.* **2009**, *8*, 1473-1483.
- [28] Z. Xia, C. Knaak, J. Ma, Z. M. Beharry, C. McInnes, W. Wang, A. S. Kraft, C. D. Smith, *J. Med. Chem.* **2009**, *52*, 74-86.
- [29] a) L. Xu, Y.-C. Meng, P. Guo, M. Li, L. Shao, J.-H. Huang, *Pharmaceutical Fronts* **2022**, *04*, e207-e222; b) S. Fujii, S. Nakamura, A. Oda, H. Miki, H. Tenshin, J. Teramachi, M. Hiasa, A. Bat-Erdene, Y. Maeda, M. Oura, M. Takahashi, M. Iwasa, I. Endo, S. Yoshida, K. I. Aihara, K. Kurahashi, T. Harada, K. Kagawa, M. Nakao, S. Sano, M. Abe, *Br J Haematol* **2018**, *180*, 246-258.
- [30] a) A. Rathi, D. Kumar, G. M. Hasan, M. M. Haque, M. I. Hassan, *Biochimica et Biophysica Acta (BBA) - General Subjects* **2021**, *1865*, 129995; b) M. C. Nawijn, A. Alendar, A. Berns, *Nat. Rev. Cancer* **2011**, *11*, 23-34.
- [31] V. Josef, F. Hampel, H. Dube, *Angew. Chem. Int. Ed.* **2022**, *61*, e202210855.
- [32] S. Luszczak, C. Kumar, V. K. Sathyadevan, B. S. Simpson, K. A. Gately, H. C. Whitaker, S. Heavey, *Signal Transduct Target Ther* **2020**, *5*, 7.
- [33] V. Asati, S. K. Bharti, A. K. Budhwani, *J. Mol. Struct.* **2017**, *1133*, 278-293.